Adult spiders use tougher silk: ontogenetic changes in web architecture and silk biomechanics in the orb-weaver spider

A. T. Sensenig[1], I. Agnarsson[2] & T. A. Blackledge[3]

1 Department of Biology, Tabor College, Hillsboro, KS, USA
2 Department of Biology, University of Puerto Rico-Río Piedras, San Juan, PR, USA
3 Department of Biology and Integrated Bioscience Program, University of Akron, Akron, OH, USA

Abstract

Body size increases greatly during ontogeny in most animals and is often accompanied by dramatic shifts in foraging strategies and hence food resources. Orb-weaver spiders provide an interesting case, where a relatively homogeneous foraging strategy, aerial silk webs, is employed across all ontogenetic stages. Orb webs are spun soon after spiders emerge from the egg sac through growth of up to two orders of magnitude in body size. The sizes of prey targeted by the spiders are also likely to increase as spiders develop. Here, we examine how relative silk investment, web architecture, and the material properties of silk in webs change during ontogeny in the orb-weaver *Neoscona arabesca*. We also quantify two emergent properties of web performance – prey stopping potential and stickiness. We find that silk investment increases isometrically with body size, with the exception of greater than expected glue production in larger spiders. Larger spiders spin larger webs, with smaller radii, but the increased volume of all silk types and greater toughness of the capture spiral silk result in the isometric scaling of stopping potential. The strength and toughness of sticky capture spiral thread increases with diameter and hence also with ontogeny, a size scaling pattern that mirrors an evolutionary pattern across spider species. Dragline thread material properties do not change over ontogeny. The improved material properties of capture spiral threads and the increased absolute stopping potential of webs are consistent with the hypothesis that rare, large prey items play a crucial role in spiders reaching adulthood and in maximizing fecundity of female orb-weaver spiders.

Introduction

Body size increases dramatically during ontogeny in most animals, often coinciding with changes in how they obtain food. Because foraging behaviors generally reflect tradeoffs that maximize fitness (Diamond, 1984; Krebs & Davies, 1997), such ontogenetic shifts in foraging behaviors therefore likely reflect changes in the costs and benefits during development (Higgins, 1995). Some organisms dramatically shift foraging strategies during development by utilizing novel food resources. For instance, amphibians that undergo complete metamorphosis, such as frogs and toads, are often herbivorous as larvae but carnivorous as adults (Altig, Whiles & Taylor, 2007). Similarly, many insect larvae are herbivorous but collect nectar as adults (Lohman & Samarita, 2009). Trophic shifts during development may be more subtle in species lacking the radical morphological changes of such holometabolous species. For instance, most orb-weaver spiders employ a relatively homogeneous foraging strategy of using sticky orb webs to capture flying insects during growth that can span a 100-fold increase in size (Prenter, Elwood & Montgomery, 1999). The type and size

of prey captured by spiders may change dramatically during such growth. Here, we test the hypotheses that orb webs exhibit allometric changes in web architecture and silk biomechanics during spider growth.

Both the material properties of silk and the architectural arrangement of threads within webs vary among spiders (Craig, 1987; Griswold *et al.*, 1998; Opell & Bond, 2001; Swanson, Blackledge & Hayashi, 2007; Harmer *et al.*, 2011; Sensenig, Agnarsson & Blackledge, 2010). Orb spiders utilize two types of fibrous silks as the primary structural components of webs (Comstock, 1940) (Fig. 1). Major ampullate (MA) dragline silk provides a dry, stiff framework of radial threads upon which a highly elastic capture spiral is attached. The capture spiral, exuded from a different set of glands, consists of an adhesive coating of aggregate silk glue surrounding a core pair of flagelliform (Flag) fibers. Both MA and Flag silk are incredibly tough energy absorbing biomaterials, but they also exhibit extraordinary differences. Flag capture spiral silks are typically 10 times more extensible than MA dragline silks (Denny, 1976; Blackledge & Hayashi, 2006). Furthermore, the extensibility of Flag silk varies about threefold among species, while
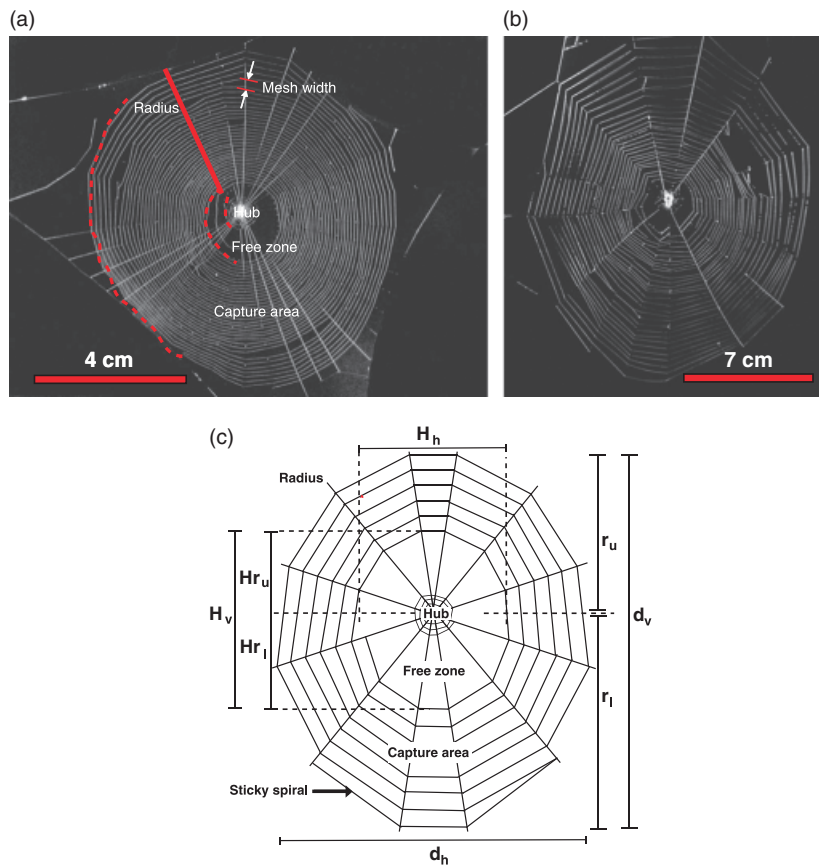
(a)

(b)

(c)

Figure 1 *Neoscona arabesca* orb webs over the ontogenetic range examined in this study. (a) Juvenile web (5 mg body weight). (b) Adult female web (38 mg body weight). (c) Web parameters used for computation of the capture spiral length (CTL).

tensile strength varies about 10-fold (Swanson *et al.*, 2007; Sensenig *et al.*, 2010). Web spinning behaviors are equally diverse. Spiders control the diameters of silk fibers (Blackledge, Cardullo & Hayashi, 2005; Boutry & Blackledge, 2008), the overall sizes of webs, (Krink & Vollrath, 2000), web stickiness (Agnarsson & Blackledge, 2009) and the spacing of silk threads within webs (Sandoval, 1994), all of which can strongly influence prey size and capture rates (Opell, 1996; Blackledge & Zevenbergen, 2006; Blackledge & Eliason, 2007). Orb webs function during prey capture in a three step process – initially intercepting flying insects, then dissipating their tremendous kinetic energy and finally adhering to insects long enough for the spiders to subdue their prey (Eberhard, 1990b). The ability of webs to dissipate kinetic energy of prey is relatively easily quantifiable and is particularly interesting because it depends on both the concentration of silk in areas of prey impact and the quality of silk threads (Sensenig *et al.*, 2010). This 'stopping potential', or maximal energy absorbed per area, is an emergent property of webs dependent on both the intrinsic quality of silks and web architecture.

Most orb-weaver spiders build their first prey capture webs soon after emerging from the egg sac, and females continue to do so throughout their adult lives. Spiderlings spin complete orbs at the first attempt and presumably use the same types of silk in approximately the same relative quantities as the silks in adult webs (Edmunds, 1993). Yet,

large spiders' webs typically capture radically larger prey than those of juveniles. The adult web must also support the large weight of the adult spider. We previously showed increases in both the amount and quality of the silk used to build webs as spiders evolve larger body sizes (Sensenig *et al.*, 2010). These changes equip bigger spider species to catch larger prey. Here, we examine whether similar scaling occurs ontogenetically within a species.

A variety of studies demonstrate ontogenetic changes in web architecture, with juveniles spinning more symmetric orbs and adults typically shifting to more specialized architectures (Eberhard, 1985, 1986; Heiling & Herberstein, 1999; Eberhard, Barrantes & Madrigal-Brenes, 2008; Kuntner & Agnarsson, 2009; Kuntner, Kralj-Fišer & Gregorič, 2010). For example, *Epeirotypus* pulls its orb shaped web into a cone and does so much more pronouncedly when it becomes an adult (Eberhard, 1986), which may be associated with higher energy of recoil when the web is released onto the prey. A particular *Eustala* species was more likely to incorporate a 'sawtoothed' pattern of spirals in their orb web at later ontogenetic stages (Eberhard, 1985). Orb weavers in general tend to reduce silk investment in the upper halves of orb webs as they grow, to the point that some adult webs can entirely lack capture spirals above their hubs (Witt, Rawlings & Reed, 1972; Edmunds, 1993; Japyassu & Ades, 1998; Kuntner *et al.*, 2008; Kuntner & Agnarsson, 2009; Hesselberg, 2010; Nakata, 2010). Finally,

in the cob-web spider *Latrodectus*, vestiges of the ancestral orb web can be detected only in the earliest instars (Eberhard *et al.*, 2008).

Only one study has investigated dragline silk properties across ontogeny, finding that the material properties of dragline silk safety lines were largely invariant, with only the increasing silk diameter providing support for the larger spider (Ortlepp & Gosline, 2008). Nothing is known about ontogenetic variation in capture spiral mechanics or whether such variation may interact with the ontogeny of web spinning behaviors. In this study, we assess ontogenetic changes in web architecture, silk material properties and stopping potential over a 23-fold increase in size for the orb-weaver spider *Neoscona arabesca* (Araneae: Araneidae). We test the hypotheses that spiders will invest allometrically in silk as their target prey becomes larger and associated with higher energy. We also ask whether material properties change over ontogeny and we test for changes in web performance as spiders grow.

Materials and methods

Animals

Thirty-seven individuals of *N. arabesca* were sampled in this study (Table 1). The dataset consisted of 15 sexually mature females and 22 juveniles. Three of the juveniles could be identified as subadult males, and three as subadult females, but the remaining juveniles could not be sexed, as reproductive anatomy changes dramatically only in the last two molts. Mass ranged 23-fold, from 5 to 116 mg. Our study is confined to approximately the last five instars of spiders because only silks spun by larger spiders can be analyzed with our tensile testing methods. Spiders were captured in Akron and Bath, OH, USA in August 2007, and placed in cages measuring $40 \times 40 \times 10$ cm. Relative humidity in the room containing the cages varied between 50 and 90%. Spiders were fed a small cricket every other day. Webs were constructed within 1–7 days after capture, and the silk tested within 24 h of spinning.

Web architecture measurements

Web architecture was measured from digital photographs taken from webs placed in front of a shadow box and illuminated from the sides by fluorescent lighting (Langer & Eberhard, 1969; Zschokke & Herberstein, 2005).

The total size of the capture area of a web determines the number of insects that it potentially intercepts. Capture area is delimited by the outermost sticky spirals (Fig. 1). Web

Table 1 Weights and ontogenetic classes of spiders used in study

Ontogenetic stage	Weight (mg) mean $\pm$ SD (n)
Adult female	46 ± 4 (15)
Subadult female	28 ± 9.6 (3)
Juvenile unsexed	14 ± 4.1 (16)
Subadult male	11 ± 9.6 (3)

capture area was measured directly from photographs of webs. The density of threads within webs influences the sizes of insects likely to be intercepted, and affects both the ability of webs to absorb the kinetic energy of flying insects and the effectiveness with which webs retain insects long enough to be captured by spiders (Blackledge & Zevenbergen, 2006). Therefore, we measured the number of radii in orbs and the number of spiral threads along four axes (North, South, East and West). Mesh width and the distance between adjacent capture spirals was calculated along each axis and then averaged (Herberstein & Tso, 2000)

The web hub is usually not centrally located, resulting in larger lower regions (ap Rhisiart & Vollrath, 1994). This hub asymmetry typically increases with spider size (Kuntner *et al.*, 2008), and is hypothesized to decrease the time necessary for a heavy spider to reach an insect caught in the lower capture region (Masters & Moffat, 1983; Heiling, 2004; Zschokke & Nakata, 2010). Hub asymmetry was defined in Blackledge & Gillespie (2002) as

$$\text{Hub asymmetry} = 1 - r_u/r_l$$

The variables r_u and r_l are the upper and lower radius of the web, respectively (Fig. 1a). Most orb webs are not round, but elliptical (ap Rhisiart & Vollrath, 1994; Sherman, 1994). The exaggerated vertical axis may facilitate prey capture by taking advantage of the tendency of prey to tumble downward as they struggle. Web asymmetry describes the relationship between height and width of the orb and was defined in Blackledge & Gillespie (2002) as

$$\text{Web asymmetry} = 1 - d_h/d_v$$

The variables d_h and d_v are the horizontal and vertical spans of the web, respectively (Fig. 1a). Perfectly round webs have a web asymmetry value of 0. A web asymmetry <0 indicates a web that is wider than it is tall, while web asymmetry >0 indicates a web that is taller than wide.

Silk structure

Investment of silk in a web can be quantified by measuring the size and length of threads and glue droplets. The total length of the capture spiral, typically designated as capture thread length (CTL) (Sherman, 1994) was calculated as

$$\text{CTL} = \pi(S_n)[(r_u + d_h + r_l)/4 - (Hr_u + H_h + Hr_l)/4]$$

The factor in the brackets represents the average width of the capture area and is estimated by subtracting the average free zone radius along the four cardinal axes from the average capture area radius along the four cardinal axes. S_n is the average # of spirals along the four web axes.

For each web, four dragline threads, one from each cardinal axis, were collected from webs onto cardboard holders described in Agnarsson & Blackledge (2009). To measure spiral thread diameter, the silk was collected directly onto a glass microscope slide. The glass slide caused the glue droplets to adhere and flatten, thereby securing the threads to the slide and making the core axial thread visible. Dragline and capture spiral thread diameters were measured

using polarized light microscopy (Blackledge et al., 2005) at $1000 \times$ magnification, as detailed in Agnarsson & Blackledge (2009).

The diameter of a single hypothetical thread, equivalent in cross-sectional area to the two core fibers of silk that typically compose a capture spiral thread, was calculated as

$$d_{hyp} = 2\sqrt{2}r_{ss}$$

Where r_{ss} was the measured radius of a single strand, assuming equal radius of each strand. In the rare instances in which we observed four stranded radial or capture threads, all four strands were assumed to be equal diameter. In this case:

$$d_{hyp} = 4r_{ss}$$

The average hypothetical thread diameter for a specific web and specific silk type was then calculated as the average of the four collected thread samples.

Volume of capture spiral thread was then computed as

$$V_{sp} = (CTL)\pi(d_{hyp\_sp}/2)^2$$

where V_{sp} is the total capture spiral volume, and d_{hyp_sp} is the hypothetical capture spiral diameter.

Total dragline thread volume was calculated as

$$V_{rad} = (r_u + d_h + r_l)/4(R_n)\pi(d_{hyp\_rad}/2)^2$$

where V_{rad} is total dragline thread volume, R_n is the number of radii in the web and d_{hyp_rad} is the hypothetical dragline thread diameter.

Four samples of capture spiral were taken to test stickiness, starting from the outermost spiral. To measure glue droplet volume on the capture spiral silk, threads were suspended between 3 mm diameter wooden supports, previously secured to a microscope slide (Agnarsson & Blackledge, 2009). The volume of a single droplet of glue (SDV) was calculated as:

$$SDV = (droplet\ width)^2(droplet\ length)/15$$

This formula accounts for the anisotropy of the droplet shape, which tends to be more long than wide as it adheres to the capture spiral thread (Opell et al., 2008). The average distance between glue droplets was measured across 10 adjacent droplets. Total volume of glue within the web was then calculated as

$$V_{glue} = SDV \times CTL/average\ distance\ between\ droplets$$

Biomaterial properties

We characterized the intrinsic material properties of both dragline and capture spiral silks using a Nano Bionix test system (Agilent Technologies, Oakridge, TN, USA), previously described in Blackledge, Swindeman & Hayashi (2005), Blackledge & Hayashi (2006), Agnarsson, Boutry & Blackledge (2008) and Agnarsson & Blackledge (2009). For each web, material properties of both dragline and capture spiral silk represent averages of four samples. For each silk sample, we generated force-extension curves of silk by extending silk threads at 10%/s. Stiffness, or Young's

modulus, was measured for dragline silk as the slope of the force/extension curve during the initial extension of the silk fiber, a region in which the relationship between force and extension was approximately linear (Gosline et al., 1999). At high extension for both dragline and capture spiral threads, the force rose rapidly before the fiber broke. Ultimate strength was then calculated as the amount of force required to break a fiber relative to the instantaneous cross-sectional area of the fiber, assuming constant volume during extension (Vollrath, Madsen & Shao, 2001; Guinea et al., 2006). Extensibility, or strain, was calculated as the natural log of the breaking length divided by the original length. Toughness, or the energy absorbed by a fiber before rupture, was calculated as the area under the stress–strain curve divided by the sample volume. The maximal energy a web could absorb was the sum of the toughness of each silk type multiplied by the total respective volume of each silk type. The stopping potential was defined as this maximal energy divided by the capture area (Sensenig et al., 2010). Thus, stopping potential provides a theoretical measure of the maximum performance of webs that could only be achieved if all silk deformed perfectly during prey capture. Real performance will obviously be less, but our measure of stopping potential correlates highly with actual measured performance of webs (Sensenig et al., 2010).

The third phase of prey capture (retention), requires the glue droplets of the capture spiral threads to sufficiently adhere to the prey as it struggles and hangs in the web. The sticky glue droplets on the edges of a contacted surface contribute most to adhesion, but droplets on the interior of surfaces also contribute to adhesive force, a mechanism known as the suspension bridge model (Opell & Hendricks, 2007). The total adhesive force on a particular insect will depend on the surface features of the insect and number of droplets contributing to the suspension bridge (Opell & Schwend, 2007). We quantified glue stickiness by pressing a capture spiral onto a standard 2 mm wide strip of sand paper and then measuring the force required to pull the capture silk from the sandpaper contact at a rate of $1\ mm\ s^{-1}$ (Agnarsson & Blackledge, 2009). We averaged the adhesive force of four thread samples, taken from the outermost spiral and working inward. From this average thread adhesive force, we calculated web stickiness/area, a property analogous to our estimated stopping potential criteria of energy absorbed/area. This stickiness per area was defined as

$$St_a = (F_g)(CTL)/A_c/C_g$$

St_a is the stickiness per area, F_g is the average adhesive force of the glue, C_g is the length of contact with force transducer (2 mm) and A_c is the capture area of the web.

Statistical methods

Testing for spider body condition

Spiders were weighed to the nearest milligram using a balance, and then preserved in 95% ethanol. Carapace width was then measured using a stereomicroscope equipped with

Table 2 Results of ANCOVA to determine which variables predict silk volume investment

| Independent variable | Multivariate tests of significance. Sigma-restricted parameterization | | | | | |
	Test	Value	F	Effect	Error	P
Log weight	Wilks	0.539995	7.66681	3	27	0.0007
Log carapace width	Wilks	0.726494	3.38826	3	27	0.0324
Instar	Wilks	0.966308	0.31380	3	27	0.8152

The volumes of three types of silk represented the three dependent variables in the model.

Table 3 Results of MANOVA to determine which of 18 properties change with log spider weight

	Adjusted R^2	SS model	d.f. model	MS model	SS residual	d.f. residual	MS residual	F	P
Dragline stiffness (GPa)	0.023262	10.5	1	10.5	171	27	6.32	1.667	0.21
Dragline true stress (MPa)	0.030542	183 694.2	1	183 694.2	2 635 193	27	97 599.72	1.882	0.18
Ln [dragline toughness (MPa)]	−0.000601	0.1	1	0.1	2	27	0.07	0.983	0.33
1/[dragline true strain (ln mm/mm)]	−0.032991	0.1	1	0.1	16	27	0.59	0.106	0.75
Ln [spiral strength (MPa)]	0.180705	1.4	1	1.4	5	27	0.20	7.176	0.01
spiral true strain (ln mm/mm)	0.175656	0.3	1	0.3	1	27	0.04	6.966	0.01
Ln [spiral toughness (MPa)]	0.306127	3.4	1	3.4	7	27	0.26	13.353	0.00
Log [web area (cm²)]	0.183795	0.4	1	0.4	1	27	0.05	7.305	0.01
Mesh width (mm)	0.004172	0.4	1	0.4	10	27	0.36	1.117	0.30
1/number of radials	0.203280	0.0	1	0.0	0	27	0.00	8.144	0.01
Ln (spirals/radii)	0.229776	1.0	1	1.0	3	27	0.11	9.353	0.00
Hub asymmetry	−0.032608	0.0	1	0.0	1	27	0.03	0.116	0.74
Web asymmetry	0.044114	0.0	1	0.0	0	27	0.00	2.292	0.14
Log [glue volume (mm³)]	0.586499	4.4	1	4.4	3	27	0.11	40.714	0.00
Log [dragline volume (mm³)]	0.432894	1.5	1	1.5	2	27	0.07	22.373	0.00
Log [spiral volume (mm³)]	0.513605	2.5	1	2.5	2	27	0.08	30.566	0.00
Log (energy at break/web surface area)	0.562024	3.4	1	3.4	2	27	0.09	36.930	0.00
Log (stickiness/web surface area)	0.189157	1.2	1	1.2	4	27	0.16	7.532	0.01

Gray fill indicates a significant effect of spider body weight ($P < 0.05$).

an ocular scale. Body condition index is typically calculated as the residuals of the regression of natural log body weight onto natural log carapace width (Jakob, Marshall & Uetz, 1996). More positive residuals indicate 'fatter', better body condition spiders, likely because of recent foraging success. Body condition could affect some web properties, such as silk investment (Brandwood, 1985; Ortlepp & Gosline, 2008). However, regression involving this body condition index violates several important statistical assumptions (Garcia-Berthou, 2001). Therefore, we used an analysis of covariance (ANCOVA) of the original variables in order to test for potentially independent effects of weight and size on silk production in STATISTICA 8.0 (StatSoft Inc., 2009). The dependent variables were the log of silk volume (three different silk types), while the continuous predictors were the log of body weight and log of carapace width (Table 2). The categorical predictor was ontogenetic stage (two categories: juvenile and adult).

Comparing material, architecture and emergent web performance properties across ontogeny

The effect of spider body weight on 18 properties including web architecture, silk material properties, silk masses and emergent web performance properties was tested using a Multivariate Analysis of Variance (MANOVA) in the General Linear Model option of STATISTICA 8.0 (StatSoft Inc., 2009). Spiral thread material properties included breaking strength, extensibility and toughness. Dragline thread material properties were stiffness, breaking strength, extensibility and toughness. Architecture properties were web area, mesh width, number of radii, spiral:radii ratio, web asymmetry and hub asymmetry (Table 3). Web area, capture spiral strength, capture spiral toughness, dragline thread toughness and spiral:radii ratio were natural log transformed to meet assumptions of normal distribution (Shapiro–Wilks W-test, $P > 0.05$) and homogeneous variance (Levene's test for homogeneity of variances, $P > 0.05$, d.f. 1, 21). Radii number and radial true strain were transformed by the multiplicative inverse.

Testing allometry of silk investment and web performance

After finding a significant effect of body weight on web properties in the MANOVA, we specifically addressed whether the shift differed from isometry for the three silk volumes, the web area and the two performance properties.

Isometric growth occurs when the volume of an organ increases linearly with the total weight or volume of the organism such that organism shape is consistent throughout development. Allometry is defined as the growth of organs and the whole organism at different rates (Gould, 1966). The standard allometric equation is

$$V_{sp} = (\text{body weight})^B + C$$

where V_{sp} is volume of a specific feature of interest, B defines the relationship with body weight and C is a unique constant. Taking the log of both sides:

$$\log(V_{sp}) = B \times \log(\text{body weight}) + \log(C)$$

The exponent B is now the slope of a log–log plot. If $B = 1$ then the organ (V_{sp}) is growing at an isometric rate. If $B < 1$, then the organ is growing at an allometric rate, more slowly than the organism, and $B > 1$ indicates allometric growth of the organ at a faster rate. Investment in silk resources was assessed by comparing the increase in silk volume associated with increased body size to that predicted by isometric growth. The log of silk volume (in this example, capture spiral volume) was plotted against the log of body weight. Tests for the difference between actual slopes and the null hypothesis that $B = 1$ were performed by regressing two new variables:

$$\log(\text{body weight}) + \log(V_{sp})$$
$$\text{and} \log(\text{body weight}) - \log(V_{sp})$$

(Warton *et al.*, 2006). A significant relationship between these new variables indicates that $B \neq 1$. In the case of the web capture area, we also tested whether B differed from the surface area scaling $B = 0.67$.

Once a spider enters adulthood, it may experience a selection pressure for silk investment that depends strongly on the spider size. In particular, gravid females may reduce silk investment in order to funnel protein to egg development (Higgins, 1990). This may be in addition to the overall change in investment pressure over ontogeny. Therefore, we tested for difference in the slope B of silk investment for the three silk types between adult and juvenile stages with a homogeneity of slopes ANCOVA in STATISTICA 8.0 (StatSoft Inc., 2009).

Results

Testing for spider body condition

Both spider weight ($P < 0.001$) and carapace width ($P = 0.03$) independently affected silk volume production (Table 2). Therefore, some of the web changes we find over ontogeny may be due to spider condition in addition to size scaling effects. However, ontogenetic stage did not influence silk volume, indicating that any 'poor' conditioned spiders were equally distributed across adults and juveniles.

Comparing material, architecture and emergent performance properties across ontogeny

There was an overall effect of body weight on web properties ($P = 0.002$), with 11 of 18 properties in the model changing over ontogeny (Table 3). Capture spiral tensile properties improved while dragline material properties were consistent (Table 3, Fig. 2b). Spirals were stronger (raw vs. log weight, $r = 0.37$, $P = 0.02$) (Fig. 2a), tougher (log vs. log weight, $r = 0.44$, $P < 0.01$), and increased in extensibility (raw vs. log weight, $r = 0.33$, $P = 0.04$) with spider body size. Webs increased with spider size (raw vs. log weight, $r = 0.54$, $P < 0.001$) (Fig. 3a), with the adult web area 30% larger on average than the juveniles sampled. Adult instars spun fewer
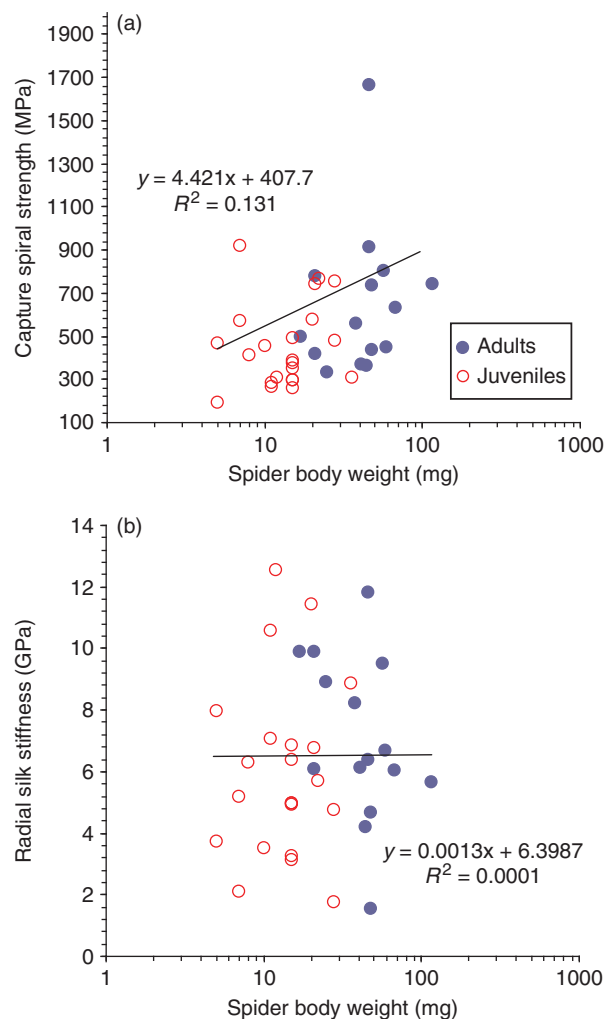

Figure 2 All the capture spiral material properties improved while all dragline properties remained constant over ontogeny. (a) Capture spiral strength increased with spider weight (Pearson's correlation, raw vs. log, $r = 0.37$, $P = 0.02$, $n = 37$). Regression of all spiders shown as solid line. (b) Dragline stiffness did not change with spider weight (Pearson's correlation, raw vs. log, $r = 0.07$, $P = 0.67$, $n = 37$). Regression of all spiders shown as solid line.
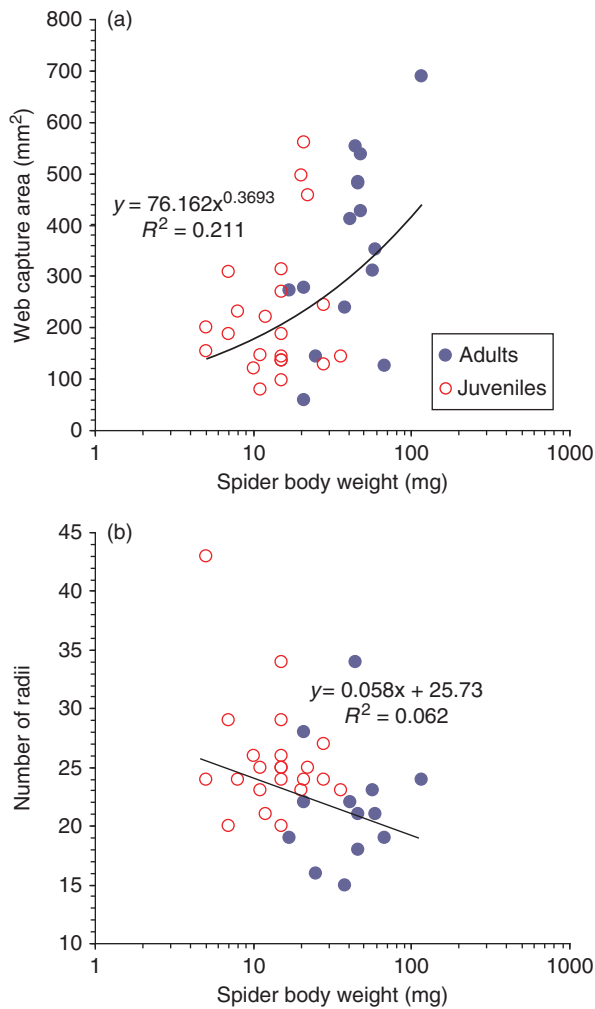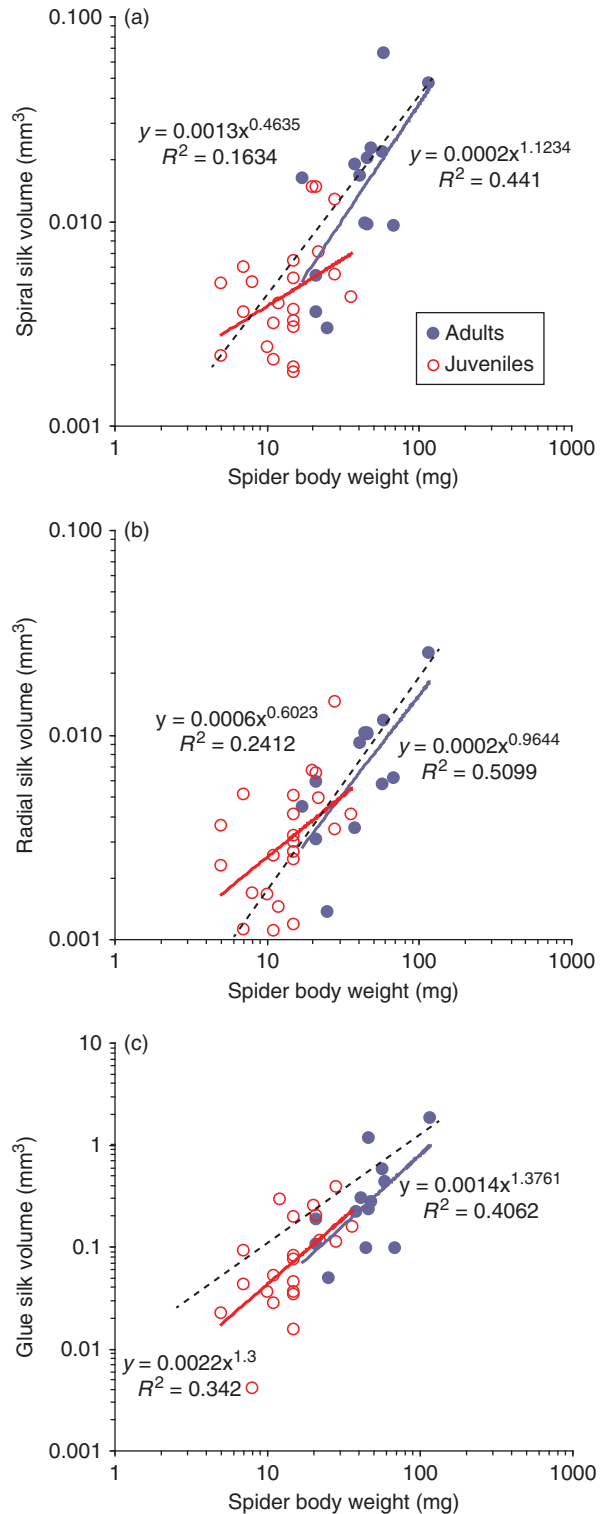
$y = 76.162x^{0.3693}$
$R^2 = 0.211$

from that predicted by isometry ($B = 1$), in this case increasing with a slope of 1.24 ($P < 0.001$) (Fig. 4c). Capture spiral silk investment increased isometrically with increasing spider size for the full set of spiders ($B = 0.87$, isometry $B = 1$, $P = 0.14$). Radial (MA) silk investment was also isometric

$y = 0.0013x^{0.4635}$
$R^2 = 0.1634$

$y = 0.0002x^{1.1234}$
$R^2 = 0.441$

$y = 0.058x + 25.73$
$R^2 = 0.062$

$y = 0.0006x^{0.6023}$
$R^2 = 0.2412$

$y = 0.0002x^{0.9644}$
$R^2 = 0.5099$

Figure 3 Some architecture features changed with spider size. (a) Web area increased with spider size (Pearson's correlation, raw-log, $r = 0.53$, $P < 0.001$, $n = 37$) with $B = 0.37$ (log–log). Power function best fit using all spiders shown as solid line. This B was less than the rate predicted by isometry, under both volume ($B = 1$) and surface area scaling assumptions ($B = 0.67$). (b) Number of radii in a web decreased with spider size (Pearson's correlation, raw vs. log, $r = -0.36$, $P = 0.03$, $n = 35$). Linear best fit using all spiders shown as solid line.

radii (raw vs. log weight, $r = -0.36$, $P = 0.03$) (Fig. 3b) and had higher ratios of capture spiral rows to radii (raw vs. log weight, $r = 0.38$, $P = 0.02$). Web (raw vs. log weight, $r = 0.24$, $P = 0.19$) and hub asymmetry (raw vs. log weight, $r = 0.04$, $P = 0.82$) did not change over ontogeny.

Testing allometry of silk investment and web performance

Larger spiders included more volume of silk in their webs. This was due to both increased overall thread length associated with larger orb webs and increased thread diameters and glue droplet sizes. Of the three silk types, only glue volume increased at a rate that significantly differed

$y = 0.0014x^{1.3761}$
$R^2 = 0.4062$

$y = 0.0022x^{1.3}$
$R^2 = 0.342$

with spider size ($B = 0.72$, isometry $B = 1$, $P = 0.44$, $n = 35$). The rate at which silk investment changed with spider body size did not differ between adults and juveniles ($P > 0.05$ for all three silk types).

The combined effects of increasing material investment, improved tensile properties, and web area produced an average 12-fold increase in stickiness per area (Fig. 5b), and 20-fold increase in stopping potential (energy absorbed per area) (Fig. 5a) over ontogeny. This corresponded to an increase in stopping potential that met isometry in larger spiders ($B = 0.69$, not significantly different from $B = 1$, $P = 0.66$, $n = 35$). In contrast, stickiness per area increased at a rate less than that predicted by isometry $B = 1$ ($B = 0.56$, $P = 0.004$, $n = 35$). The capture area of large webs was less than that predicted by isometry, under both surface area and volume scaling assumptions (Fig. 3a).

Discussion

The capture of large, but rare, prey late in spider ontogeny is a key event for reproduction and predicts a greater allocation of resources to web silk late in a spider's life (Venner & Casas, 2005; Blackledge, 2011). The higher kinetic energy prey targeted by larger spiders predicts shifts toward higher silk investment and otherwise better performing webs. However, of the three silk components of orb webs, only glue investment increased allometrically during growth. More glue increases stickiness per area and thus should increase the time that a web can retain prey (Miyashita, 1997; Agnarsson & Blackledge, 2009). Even though glue silk volume increased faster than isometry, the stickiness per area of webs increased at a rate less than that predicted by isometry. This is likely due to the wider, albeit statistically insignificant, increase in spacing of the capture spiral over ontogeny and a decrease in the relative surface area per volume of the adhesive droplets. Despite large spiders spinning relatively smaller area webs, which concentrates greater volumes of tougher silk into proportionally smaller webs (Fig. 3a), the stopping potential scaled isometrically with body weight (Fig. 5a). Capture spiral material properties improved significantly during growth to adulthood. In contrast, dragline material properties remained unchanged through ontogeny. This may indicate that dragline threads

$y = 0.7005x^{0.6887}$
$R^2 = 0.5278$

● Adults
○ Juveniles

$y = 6.3619x^{0.5613}$
$R^2 = 0.1985$

Figure 5 Whole web performance increased over ontogeny. (a) Stopping potential increased isometrically with spider weight, with $B = 0.69$, which was not significantly different from $B = 1$ ($P = 0.66$, $n = 35$). Regression of all spiders shown as solid line and isometry ($B = 1$) indicated with dashed line. (b) Stickiness per area increased at a rate lower than predicted by volume isometry with spider weight, with $B = 0.56$ ($P = 0.004$, $n = 35$). Regression of all spiders shown as solid line and isometry ($B = 1$) indicated with dashed line.

are already functioning optimally, or maximally, early in ontogeny, or that the main constraint on web function is spiral thread and glue performance. Our findings of constant dragline material properties contrast with the decline in dragline stiffness reportedly spun by spiders with artificial weights glued to the body (Vollrath & Köhler, 1996), but is similar to studies of MA silk used as a lifeline (Osaki, 1999; Ortlepp & Gosline, 2008).

Hub asymmetry shifts are prominent features of ontogeny in many spider species, such as *Larinioides cornutus* (pers. obs.), several Nephilidae genera (Japyassu & Ades, 1998; Kuntner *et al.*, 2008; Kuntner & Agnarsson, 2009), and in *Cyclosa* (Nakata & Zschokke, 2010). Therefore, it is surprising that there was no effect of ontogeny on hub asymmetry in *N. arabesca*. Hub asymmetry is most dramatic

Figure 4 (a) Capture spiral (Flag) silk investment increased isometrically with increasing spider size for the full set of spiders ($B = 0.87$, isometry $B = 1$, $P = 0.14$). Actual regressions shown as solid lines and isometry ($B = 1$) indicated with dashed line. Regression lines are solid red for juveniles and solid blue for adults, with the regression equation shown adjacent to the corresponding line. Slopes of juveniles and adults did not differ (ANCOVA, d.f. = 1,32, $F = 1.19$, $P = 0.28$, $n = 36$), although adult growth tended closer to isometry. (b) Dragline (MA) silk investment was isometric with spider size ($B = 0.72$, isometry $B = 1$, $P = 0.44$, $n = 35$). Slopes of juveniles and adults did not differ (ANCOVA, d.f. = 1,31, $F = 0.03$, $P = 0.86$). (c) Glue silk volume increased allometrically ($B = 1.24$, isometry $B = 1$, $P < 0.001$, $n = 34$) with spider weight. Slopes of juveniles and adults did not differ (ANCOVA, d.f. = 1,30, $F = 0.10$, $P = 0.76$).
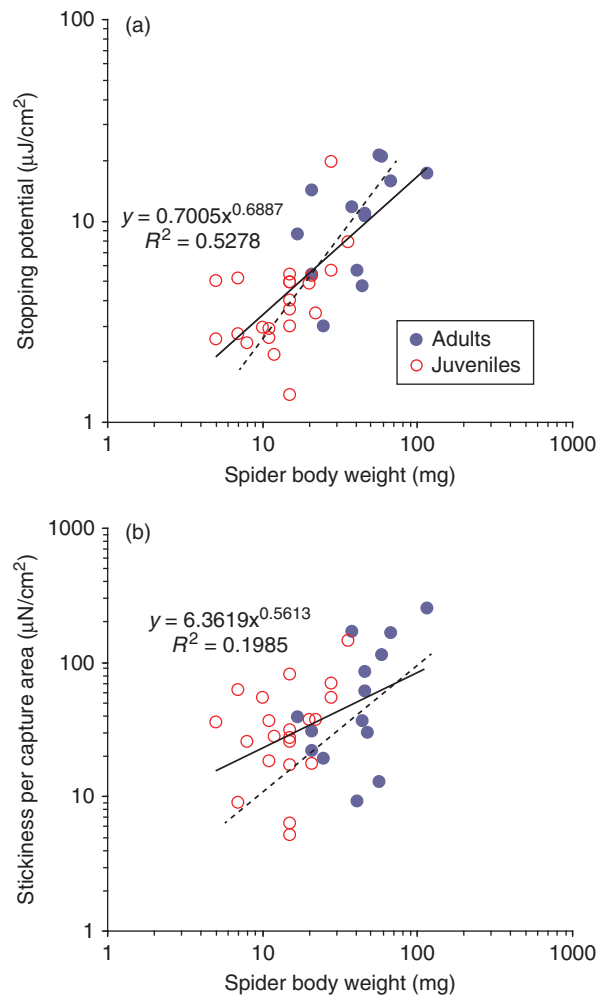
in larger spiders, and is hypothesized to enable heavy spiders to efficiently attack prey by moving downward from a high hub with the force of gravity (Masters & Moffat, 1983; Nentwig, 1985b; ap Rhisiart & Vollrath, 1994; Herberstein & Heiling, 1999; Zschokke & Nakata, 2010).

Many studies attempt to link variation in the mesh widths of webs to the sizes or taxa of targeted insect prey (e.g. Nentwig, 1985a; Eberhard, 1990a; Sandoval, 1994). However, the common prediction that larger mesh widths target larger prey is not necessarily supported (Herberstein & Heiling, 1998; Blackledge & Zevenbergen, 2006). In particular, denser capture meshes perform better at capturing large prey (Blackledge & Eliason, 2007). Therefore, even though we detected no change in mesh width in *N. arabesca*, the stopping and retention performance of the webs of larger spiders is much greater than that of the small spiders (Fig. 5a and b). In light of the 20-fold difference in stopping potential among webs of large and small spiders, similarity in mesh width is not clear evidence of webs targeting similar size prey across ontogeny. Rather, increases in the stopping and retention performance of orb webs is evidence that larger spiders are targeting bigger and faster flying prey, in part by concentrating limited silk resources.

In many holometabolous insects, larval feeding is critical to fecundity because adult insects often rely largely upon larval fat stores (Boggs & Freeman, 2005). In stark contrast, female spiders actively forage as adults during which time their prey intake correlates closely with fecundity (Venner & Casas, 2005). Our findings demonstrate changes in both web architecture and silk biomechanics during spider ontogeny. Both the stopping potential and the stickiness per area of webs increase due to the high amount of silk packed into the webs of adults, and also due to the dramatic increase in the material performance of capture spiral threads, which are stronger, stretchier and tougher in adults. The increase in capture spiral quality with spider size was previously demonstrated across species differing in size (Sensenig *et al.*, 2010), but is here for the first time documented occurring through ontogeny. Significantly, a concerted shift toward absolute high performance in larger spiders also occurs at the interspecific level (Sensenig *et al.*, 2010). This suggests that increased body size places demands on webs that are compensated by similar architectural and material changes, at both the evolutionary and ontogenetic levels. Larger spiders of *N. arabesca* build both bigger and stronger webs on the absolute scale, but smaller and equivalent strength webs when scaled to isometric predictions. While allometrically enhanced stopping potential of webs would have been strong evidence for the hypothesis that rare large prey items are essential to high fecundity of female orb-weaver spiders, the increased absolute stopping potential is still consistent with this hypothesis.

Acknowledgments

References

Agnarsson, I. & Blackledge, T.A. (2009). Can a spider web be too sticky? Tensile mechanics constrains the evolution of capture spiral stickiness in orb weaving spiders. *J. Zool. (Lond.)* **278**, 134–140.

Agnarsson, I., Boutry, C. & Blackledge, T.A. (2008). Spider silk aging: initial improvement in a high performance material followed by slow degradation. *J. Exp. Zool.* **309A**, 494–504.

Altig, R., Whiles, M.R. & Taylor, C.L. (2007). What do tadpoles really eat? Assessing the trophic status of an understudied and imperiled group of consumers in freshwater habitats. *Freshw. Biol.* **52**, 386–395.

ap Rhisiart, A. & Vollrath, F. (1994). Design features of the orb web of the spider, *Araneus diadematus*. *Behav. Ecol.* **5**, 280–287.

Blackledge, T.A. (2011). Prey capture in orb weaving spiders: are we using the best metric? *J. Arachnol.*, **39**, in press.

Blackledge, T.A., Cardullo, R.A. & Hayashi, C.Y. (2005). Polarized light microscopy, variability in spider silk diameters, and the mechanical characterization of spider silk. *Invertebr. Biol.* **124**, 165–173.

Blackledge, T.A. & Eliason, C.M. (2007). Functionally independent components of prey capture are architecturally constrained in spider orb webs. *Biol. Lett.* **3**, 456–458.

Blackledge, T.A. & Gillespie, R.G. (2002). Estimation of capture areas of spider webs in relation to web asymmetry. *J. Arachnol.* **30**, 70–77.

Blackledge, T.A. & Hayashi, C.Y. (2006). Silken toolkits: biomechanics of silk fibers spun by the orb web spider *Argiope argentata*. *J. Exp. Biol.* **209**, 2452–2461.

Blackledge, T.A., Swindeman, J.E. & Hayashi, C.Y. (2005). Quasistatic and continuous dynamic characterization of the mechanical properties of silk from the cobweb of the black widow spider *Latrodectus hesperus*. *J. Exp. Biol.* **208**, 1937–1949.

Blackledge, T.A. & Zevenbergen, J.M. (2006). Mesh width influences prey retention in spider orb webs. *Ethology* **112**, 1194–1201.

Boggs, C. & Freeman, K. (2005). Larval food limitation in butterflies: effects on adult resource allocation and fitness. *Oecologia* **144**, 353–361.

Boutry, C. & Blackledge, T.A. (2008). The common house spider alters the material and mechanical properties of cobweb silk in response to different prey. *J. Exp. Zool.* **309A**, 542–552.

Brandwood, A. (1985). Mechanical properties and factors of safety of spider drag-lines. *J. Exp. Biol.* **116**, 141–151.

Comstock, J.H. (1940). *The spider book*. Ithaca: Comstock Publishers.

Craig, C.L. (1987). The significance of spider size to the diversification of spider-web architectures and spider reproductive modes. *Am. Nat.* **129**, 47–68.

Denny, M. (1976). Physical properties of spider's silks and their role in design of orb-webs. *J. Exp. Biol.* **65**, 483–506.

Diamond, J.M. (1984). Behavioral ecology – optimal foraging theory tested. *Nature* **311**, 603–604.

Eberhard, W., Barrantes, G. & Madrigal-Brenes, R. (2008). Vestiges of an orb-weaving ancestor? The "biogenetic law" and ontogenetic changes in the webs and building behavior of the black widow spider *Latrodectus geometricus* (Araneae Theridiidae). *Ethol. Ecol. Evol.* **20**, 211–244.

Eberhard, W.G. (1985). The "sawtoothed" orb web of *Eustala* sp. (Araneae, Araneidae) with a discussion of ontogenetic changes in spiders' web-building behavior. *Psyche* **92**, 105–117.

Eberhard, W.G. (1986). Ontogenic changes in the web of *Epeirotypus* sp. (Araneae, Theridiosomatidae). *J. Arachnol.* **14**, 125–128.

Eberhard, W.G. (1990a). Early stages of orb construction by *Philoponella vicina*, *Leucauge mariana*, and *Nephila clavipes* (Araneae, Uloboridae and Tetragnathidae), and their phylogenetic implications. *J. Arachnol.* **18**, 205–234.

Eberhard, W.G. (1990b). Function and phylogeny of spider webs. *Annu. Rev. Ecol. Syst.* **21**, 341–372.

Edmunds, J. (1993). The development of the asymetrical web of *Nephilengys cruentata* (Fabricius). *Mem. Queensl. Mus.* **33**, 503–506.

Garcia-Berthou, E. (2001). On the misuse of residuals in ecology: testing regression residuals vs. the analysis of covariance. *J. Anim. Ecol.* **70**, 708–711.

Gosline, J.M., Guerette, P.A., Ortlepp, C.S. & Savage, K.N (1999). The mechanical design of spider silks: from fibroin sequence to mechanical function. *J. Exp. Biol.* **202**, 3295–3303.

Gould, S.J. (1966). Allometry and size in ontogeny and phylogeny. *Biol. Rev.* **41**, 587–638.

Griswold, C.E., Coddington, J.A., Hormiga, G. & Scharff, N. (1998). Phylogeny of the orb-web building spiders (Araneae, Orbiculariae: Deinopoidea, Araneoidea). *Zool. J. Linn. Soc.* **123**, 1–99.

Guinea, G.V., Pérez-Rigueiro, J., Plaza, G.R. & Elices, M. (2006). Volume constancy during stretching of spider silk. *Biomacromolecules* **7**, 2173–2177.

Harmer, A.M.T., Blackledge, T.A., Madin, J.S. & Herberstein, M.E. (2011). High-performance spider webs: integrating biomechanics, ecology and behaviour. *J. Roy. Soc. Inter.* **8**, 457–471.

Heiling, A.M. (2004). Effect of spider position on prey capture success and orb-web design. *Acta Zool. Sin.* **50**, 554–565.

Heiling, A.M. & Herberstein, M.E. (1999). The role of experience in web-building spiders (Araneidae). *Anim. Cogn.* **2**, 171–177.

Herberstein, M.E. & Heiling, A.M. (1998). Does mesh height influence prey length in orb-web spiders (Araneae)? *Eur. J. Entomol.* **95**, 367–371.

Herberstein, M.E. & Heiling, A.M. (1999). Asymmetry in spider orb webs: a result of physical constraints? *Anim. Behav.* **58**, 1241–1246.

Herberstein, M.E. & Tso, I.M. (2000). Evaluation of formulae to estimate the capture area and mesh height of orb webs (Araneoidea, Araneae). *J. Arachnol.* **28**, 180–184.

Hesselberg, T. (2010). Ontogenetic changes in web design in two orb-web spiders. *Ethology* **116**, 535–545.

Higgins, L. (1990). Variation in foraging investment during the intermolt interval and before egg-laying in the spider *Nephila clavipes*. *J. Insect Behav.* **3**, 773–783.

Higgins, L.E. (1995). Direct evidence for trade-offs between foraging and growth in a juvenile spider. *J. Arachnol.* **23**, 37–43.

Jakob, E.M., Marshall, S.D. & Uetz, G.W. (1996). Estimating fitness: a comparison of body condition indices. *Oikos* **77**, 61–67.

Japyassu, H.F. & Ades, C. (1998). From complete orb to semi-orb webs: Developmental transitions in the web of *Nephilengys cruentata* (Araneae : Tetragnathidae). *Behaviour* **135**, 931–956.

Krebs, J.R. & Davies, N.B. (1997). *Behavioral ecology: an evolutionary approach*. Malden: Blackwell Science Ltd.

Krink, T. & Vollrath, F. (2000). Optimal area use in orb webs of the spider. *Araneus diadematus*. *Naturwissenschaften* **87**, 90–93.

Kuntner, M. & Agnarsson, I. (2009). Phylogeny accurately predicts behaviour in Indian Ocean *Clitaetra* spiders (Araneae: Nephilidae). *Invertebr. Syst.* **23**, 193–204.

Kuntner, M., Haddad, C.R., Aljancic, G. & Blejec, A. (2008). Ecology and web allometry of *Clitaetra irenae*, an arboricolous african orb-weaving spider (Araneae, Araneoidea, Nephilidae). *J. Arachnol.* **36**, 583–594.

Kuntner, M., Kralj-Fišer, S. & Gregorič, M. (2010). Ladder webs in orb-web spiders: ontogenetic and evolutionary patterns in Nephilidae. *Biol. J. Linn. Soc.* **99**, 849–866.

Langer, R.M. & Eberhard, W. (1969). Laboratory photography of spider silk. *Am. Zool.* **9**, 97–101.

Lohman, D.J. & Samarita, V.U. (2009). The biology of carnivorous butterfly larvae (Lepidoptera: Lycaenidae: Miletinae: Miletini) and their ant-tended hemipteran prey in Thailand and the Philippines. *J. Nat. Hist.* **43**, 569–581.

Masters, W.M. & Moffat, A.J.M. (1983). A functional explanation of top-bottom asymmetry in vertical orb webs. *Anim. Behav.* **31**, 1043–1046.

Miyashita, T. (1997). Factors affecting the difference in foraging success in three co-existing *Cyclosa* spiders. *J. Zool.* **242**, 137–149.

Nakata, K. (2010). Does ontogenetic change in orb web asymmetry reflect biogenetic law? *Naturwissenschaften* **97**, 1029–1032.

Nakata, K. & Zschokke, S. (2010). Upside-down spiders build upside-down orb webs: web asymmetry, spider orientation and running speed in *Cyclosa*. *Proc. Roy. Soc. Lond. B.* **277**, 3019–3025.

Nentwig, W. (1985a). Prey analysis of four species of tropical orb-weaving spiders (Araneae, Araneidae) and a comparison with araneids of the temperate zone. *Oecologia* **66**, 580–594.

Nentwig, W. (1985b). Top-bottom asymmetry in vertical orbwebs: a functional explanation and attendant complications. *Oecologia* **67**, 111–112.

Opell, B.D. (1996). Functional similarities of spider webs with diverse architectures. *Am. Nat.* **148**, 630–648.

Opell, B.D. & Bond, J.E. (2001). Changes in the mechanical properties of capture threads and the evolution of modern orb-weaving spiders. *Evol. Ecol. Res.* **3**, 567–581.

Opell, B.D. & Hendricks, M.L. (2007). Adhesive recruitment by the viscous capture threads of araneoid orb-weaving spiders. *J. Exp. Biol.* **210**, 553–560.

Opell, B.D., Markley, B.J., Hannum, C.D. & Hendricks, M.L. (2008). The contribution of axial fiber extensibility to the adhesion of viscous capture threads spun by orb-weaving spiders. *J. Exp. Biol.* **211**, 2243–2251.

Opell, B.D. & Schwend, H.S. (2007). The effect of insect surface features on the adhesion of viscous capture threads spun by orb-weaving spiders. *J. Exp. Biol.* **210**, 2352–2360.

Ortlepp, C. & Gosline, J.M. (2008). The scaling of safety factor in spider draglines. *J. Exp. Biol.* **211**, 2832–2840.

Osaki, S. (1999). Is the mechanical strength of spider's draglines reasonable as lifeline? *Int. J. Biol. Macromol.* **24**, 283–287.

Prenter, J., Elwood, R.W. & Montgomery, W.I. (1999). Sexual size dimorphism and reproductive investment by female spiders: a comparative analysis. *Evolution* **53**, 1987–1994.

Sandoval, C.P. (1994). Plasticity in web design in the spider *Parawixia bistriata* – a response to variable prey type. *Funct. Ecol.* **8**, 701–707.

Sensenig, A., Agnarsson, I. & Blackledge, T.A. (2010). Behavioural and biomaterial coevolution in spider orb webs. *J. Evol. Biol.* **23**, 1839–1856.

Sherman, P.M. (1994). The orb web - an energetic and behavioral estimator of a spiders dynamic foraging and reproductive strategies. *Anim. Behav.* **48**, 19–34.

StatSoft Inc. (2009). *STATISTICA (data analysis software system)*. Tulsa: StatSoft Inc.

Swanson, B.O., Blackledge, T.A. & Hayashi, C.Y. (2007). Spider capture silk: performance implications of variation in an exceptional biomaterial. *J. Exp. Zool. A: Ecol. Gen. Phys.* **307A**, 654–666.

Venner, S. & Casas, J. (2005). Spider webs designed for rare but life-saving catches. *Proc. Roy. Soc. Lond. B.* **272**, 1587–1592.

Vollrath, F. & Köhler, T. (1996). Mechanics of silk produced by loaded spiders. *Proc. Roy. Soc. Lond. Ser. B Biol. Sci.* **263**, 387–391.

Vollrath, F., Madsen, B. & Shao, Z.Z. (2001). The effect of spinning conditions on the mechanics of a spider's dragline silk. *Proc. Roy. Soc. Lond. B* **268**, 2339–2346.

Warton, D.I., Wright, I.J., Falster, D.S. & Westoby, M. (2006). Bivariate line-fitting methods for allometry. *Biol. Rev.* **81**, 259–291.

Witt, P.N., Rawlings, J.O. & Reed, C.F. (1972). Ontogeny of web-building behavior in two orb-weaving spiders. *Am. Zool.* **12**, 445–454.

Zschokke, S. & Herberstein, M.E. (2005). Laboratory methods for maintaining and studying web-building spiders. *J. Arachnol.* **33**, 205–213.

Zschokke, S. & Nakata, K. (2010). Spider orientation and hub position in orb webs. *Naturwissenschaften* **97**, 43–52.